Dynamics of Electrically Charged Evaporating Sprays

Laoonual Y., Stevens N., and Shrimpton J. S.

Department of Mechanical Engineering,
Imperial College London,
United Kingdom

The use of electric charge is investigated as an independent variable with which to tune fuel spray characteristics without effecting fuel metering with a view to improving DISI engine operation. Three spray charge levels (i.e. 0, 5 and 10 C/m^3) are applied to an isothermal spray with 'early' and 'late' injection strategies. The advantages gained from the use of electrically charged sprays and the influence of ambient pressure for instance the effect of moving injection timing from the intake to the compression stoke on any such advantage is investigated.

1. Introduction

With advances in electronic fuel injection control technology the interest in direct injection spark ignition (DISI) engines has been reignited. To make the most use of the possible efficiency benefits, fuel needs to be injected into either the air intake stroke, during full load engine operation or, for part load operation, into the compression stroke [1]. The ambient gas condition in the cylinder, into which the liquid fuel is to be injected, therefore varies from near ambient temperature and pressure to those conditions caused by the near adiabatic compression of this ambient air charge during the compression stroke.

The gas density increase for late fuel injection causes a reduction in the rate of liquid dispersion in the cylinder and modifies the primary atomization of the fuel [2]. The most important problem however is the reduction in time available for the spray evaporation process. This, as discussed elsewhere [3] is a strong function of engine speed and injection timing variables.

Clearly, sprays of different character are desired for different ambient conditions for different injection timings, and therefore some independent parameter is required to 'tune' the spray to the desired characteristics. In addition with the present application of DISI engines, in view of the severe timescale restraints upon drop evaporation during late injection, this tuning parameter should also accelerate global spray evaporation rates.

Together, atomizer injection pressure and fuel injection duration control fuel metering, and the former also has great influence upon the primary atomization and fuel spray dispersal rate. Since injection pressure is not independent, it cannot be used to tune spray characteristics, without effecting fuel metering.

Here the use of electric charge is investigated as an independent variable with which to influence a number of spray characteristics, and all to the benefit of engine operation. The idea is not new, indeed research elsewhere [4-5] has demonstrated the feasibility of electrostatic atomization to transient sprays of insulating liquids. Firstly dispersion characteristics of the spray may be enhanced. For isothermal sprays with no secondary atomization, the amounts of electric charge is not excessive [6] and typically spray charge densities of 5 to 10 C/m^3 are optimal to disperse the fuel without driving too much liquid onto

the cylinder walls and the piston crown. To extend the analysis provided in [6] to transient evaporating charged sprays an extension to the momentum equation, and additional variables require conservation and decisions have to be made as to how to transfer of electrical charge between the discrete and continuum phases.

2. Charged Drop Physics

A stationary drop will not be able to maintain its integrity if the drop charge exceeds the Rayleigh Limit [7]

$$Q = p\left(e_o s\right)^{1/2}\left(2D\right)^{3/2} \tag{1}$$

When the electric field is equal to the breakdown strength of the liquid, the Rayleigh limit remains valid, providing the drop doe s not discharge charge directly to the continuum, via a corona mechanism. The electric field at the drop surface is defined by

$$E = \frac{Q}{pe_o D^2} \tag{2}$$

where e_o is permittivity of the surrounding continuum. The critical diameter is therefore defined as the diameter corresponding to a drop at the Rayleigh limit and the breakdown field, e.g.

$$D_e = \frac{8s_T}{e_o E^2} \tag{3}$$

For isooctane, E ~ 1.4x10^8 V/m [8], giving D_e ~1 μm. Since D_e is small, no explicit model is used and when a drop diameter reached D_e, all mass, energy and charge is donated to the continuum.

Non-stationary Drops (without electric charge) are known to become unstable when disturbance forces, due to the pressure distribution around the drop, exceed the restorative forces due to surface tension [9]. Their behaviour may be characterised by drop Weber number, *We*, and for viscous drop, the Ohnesorge number, *Oh*,

$$We = \frac{w^2 Dr_G}{s} \;;\; Oh = \frac{m}{\sqrt{r s D}} \tag{4}$$

Several empirical models have been proposed [10-12] for primarily applications to IC engine sprays their use is perhaps the only reasonable approximation to allow the effect of secondary atomization to effect global spray properties such as penetration, dispersion and evaporation. It seems reasonable to assume that the presence of electric charge reduces the stability of drops with adverse surface pressure distributions. This was demonstrated earlier by Cerkanowicz [13]. Here, it is proposed to modify the Reitz and Diwakar model [10] to include the effect of electric charge. This is accomplished by deriving an effective surface tension term, by first noting that surface tension and electrical force, for a sphere, at the surface exactly oppose each other.

Therefore the effective surface force in the absence of tangential pressure gradients may be defined

$$F^* = 4p sD - \frac{Q^2}{2pe_o D^2} \tag{5}$$

The key modification is to the stability criteria via an effective surface tension.

$$s^* = s - \frac{Q^2}{(4p)^2 e_o D^3} \tag{6}$$

where, for σ*= 0, the Rayleigh charge (Eq. 2) may be recovered.

In the Reitz and Diwakar secondary atomization model, the stability criteria for bag and strip break-up modes occur when

$$\text{Bag: } We = \frac{r_G w^2 D}{s} > \mathbf{12} : \text{Strip: } \frac{We}{\sqrt{Re}} > \mathbf{1} \qquad (7)$$

respectively, where w is the relative velocity between the drop and the gas and Reynolds number, $Re = r_G wD/m_G$.

The lifetimes of the unstable drops corresponding to bag and stripping modes are

$$t_{bag} = C_1 \left[\frac{r_d (D)^3}{\mathbf{8}s} \right]^{1/2} : t_{strip} = C_2 \frac{D}{\mathbf{2}w} \left(\frac{r_d}{r_G} \right)^{1/2} \text{ respectively.} \qquad (8)$$

The time t_{bag} is assumed to be proportional to the drop natural frequency with the constant C_1=p. The constant C_2 is of order unity [10]

Clearly the secondary atomization rates for charged sprays are enhanced in both modes, and this may be expected to produce an enhanced rate of evaporation due to more available surface area. For IC engine applications together with the enhanced dispersion due to the space charge distribution some advantages in using charged sprays appear to be present.

The question that is to be answered however, is how much advantage is there, and how does this advantage change going to higher pressures, for instance moving from (for DISI engine) injection in the intake to injection in the compression stroke.

3. Conservative mass and charge injection

For electrically charged spray systems, integrated conservation properties such as mass and charge flow rate are easily measured. Within these conserved variables however, it is impossible to define a drop size pdf with any specific drop charge relationship, eg

$$Q = AD^n \qquad (9)$$

Where A and n are empirical constants. Clearly for a Rayleigh Limit based on charge law [7] n=1.5, $A = \mathbf{4}p\left(e_o s/\mathbf{2}\right)^{1/2}$ and for corona bombardment [14] n=2, $A = \mathbf{1}/pe_o$. Here the choice is made to define a drop pdf and not constrain the absolute drop charge, but the relative charge levels, using the following procedure.

For the time varying mass and charge flow rate $\dot{m}$ and $\dot{Q}$, over a short of time, Dt, the mass and charge added to the domain are $\dot{m}Dt$ and $\dot{Q}Dt$ respectively. During this time interval K parcels of drop are added to the domain where the k_{th} parcel contains N_k identical drops of properties D_k, T_k, Q_k, $\boldsymbol{U}_k$, $\boldsymbol{X}_k$ and the physical properties that arise from the correlations. Initially (D_k, N_k) is the kth sample of K samples from an assumed drop size pdf, and N_k is converted to the actual number by mass conservation.

Second a drop relative charge law is defined

$$\frac{Q_k}{Q_{k+1}} = \left(\frac{D_k}{D_{k+1}} \right)^n \qquad (10)$$

This allows all drop parcels charges injected in any time interval to be expressed in terms of any one charge, i.e. using Q_1,

$$\dot{Q}Dt = \sum_{k=1}^{K} N_k q_k = q_1 \sum_{k=1}^{K} N_k \left(\frac{D_k}{D_1} \right)^n \qquad (11)$$

Re-applying Eq. (10), using the value from Q_1 permits other charges from Q_k ?1 drop charges to be defined conservatively, and though not necessarily obeying the Rayleigh limit.

4. The continuum & discrete phase mathematical model

In general, the continuum fluid through which the liquid spray is dispersed is compressible and turbulent, here modelled using a standard high Reynolds number turbulence model [15] with a correction for compressible fluids [16]. In addition, for the present investigation conservation equations for voltage and for ion concentration (in the fluid continuum) are required. Treatment of the latter two conserved variables is provided in full elsewhere [17], and a repetition of the continuum phase equations is omitted for sake of brevity. The continuum phase mass, momentum, energy, fuel vapour mass fraction, voltage and ion concentration are coupled through the terms S_m^p, S_u^p, S_h^p, S_f^p and S_j^p. In addition, the $\overline{r} f_i$ term, the Lorentz force density, represents momentum transferred to the continuum through the interaction of the electric field and the ion concentration and couples the ion concentration and the electric field. The voltage is defined both by the space charge distribution of the ions in the air and the charge present upon the drops and strongly influences the ion concentration. Generation/dissipation of the turbulence due to the spray is neglected for the present.

The discrete phase which many of liquid drops comprise the sprays is described in the appendix for momentum/position, energy and mass equations.

5. Boundary conditions and geometry

The geometry is taken to be cylindrical domain of Z_{max} = 0.05m, R_{max} = 0.04 and this is discretized using a non uniform mesh of 61x41 nodes, concentrated around the spray injection point, at Z = 0, R = 250 μm. At the cylinder axis, zero gradients of all variables are assumed, and the radial velocity is zero. The three remaining boundaries are assumed to be zero voltage walls and are 'adiabatic' in terms of energy and vapour, but do act as a sink for free corona charge. A standard wall function [15] is used to model the turbulent boundary layer structure and these walls also act as perfect sinks for liquid mass, energy, and momentum, i.e. there is no rebound or shattering.

An initial condition for air depends upon the crank angle after top dead centre that the spray injection starts. Two injection timing 0-180^o CA and 300^o CA are simulated by P_o = 1 bar, T_o = 343 K and P_o=5.9 bar, T_o=570 K, and represent injection into intake and late compression stroke conditions respectively.

The liquid fuel is taken to be pure isooctane, and is injected, at a rate of 0.01 kg/s, for a time period of 1 ms, at temperature of 300 K. Mean axial velocity is defined as 70 m/s, and mean radial velocity ramps from zero to 50 m/s during 0.1 ms after the start of injection, and remains constant thereafter. In addition a fluctuation of magnitude 5% of the instantaneous mean spray injection speed is added to the initial particle velocity vector via a Gaussian random number generator of zero mean and unit variance to simulate the stochastic nature of primary atomization process. The sheet break-up point also varies stochastically and its mean position was defined as 1 mm downstream of the atomizer exit and 0-3 mm from the edge of the orifice exit, away from the centreline. Lastly the drop size and probability is sampled from an assumed pdf, taken from the dataset presented elsewhere [3]. Three spray charge levels were investigated Q_v = 0, 5 and 10 C/m^3 which reflect the useful magnitudes estimated elsewhere [3].

6. Results & Discussion

Figure 1 shows the non-dimensional mass of fuel as function of non-dimensional time. The mass fraction is normalised by the maximum observed mass while non-dimensional time is normalised by the injection duration, t_{inj}, where t_{inj} = 1 ms. First the long dashed lines, 'live mass', represents the mass of spray suspended in the gas. Secondly the solid line, 'hit mass', represents the mass fraction of spray that has hit the cylinder wall. Lastly the short dashed lines, 'evaporated mass', is the mass of evaporated spray. The sum of the three mass fractions is equal to unity. As mentioned earlier three charge levels are applied to the liquid namely no charge, 5 C/m^3, and 10 C/m^3.

Figure 1(a) shows the effect of the electric charge for an early injection at gas pressure of 1 bar. The non-charged spray does not evaporate much at the low pressure. Due to this low evaporation rate, the graphs of 'live mass' and 'hit mass' appear to be mirror images of each other. The 5 and 10 C/m^3 electric charge begins to have a significant effect on spray behaviour at 4 ms and 2 ms aSOI respectively. With a charge of 10 C/m^3 the 'live mass' reduces dramatically and is equal to the 'hit mass' at 8 ms aSOI. Therefore in the case of the early injection using electric charge, the higher electric charge reduces the existance timescale of the liquid as a result of driving too much liquid onto the cylinder wall and perhaps the piston crown.

Figure 1(b) shows the effect of the electric charge for a late injection at gas pressure of 6 bar. At this high pressure the spray evaporates quicker due to the higher ambient temperature assumption which can be seen in Fig. 1(b) as the graphs of 'evaporated mass' increase rapidly after the start of injection. In the case of non-charged spray, 90% of the liquid is evaporated within 3 ms aSOI. The electric charge helps to reduce the evaporation timescale. For example, with an electric charge of 10 C/m^3, 90% of the liquid is evaporated within 2 ms aSOI which is 1 ms quicker than non-charged spray, although a small amount of liquid is deposited on to the cylinder wall. The spray reaches a completely evaporated condition at approximately 3, 4 and 8 ms aSOI for charge level of 10, 5 and no charge respectively.

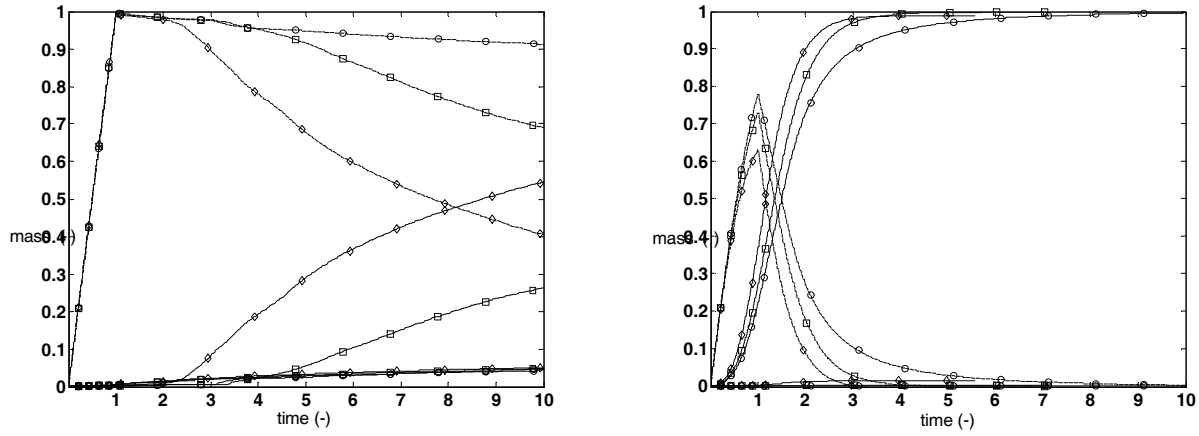

Fig. 1 The normalised mass: — — — live mass, —— hit mass, and – – – evaporate mass, as a function of normalised time by injection time, t_{inj}, where t_{inj} = 1ms, with effects of ambient pressure (a) P_o = 1 bar, and (b) P_o = 6 bar and charge levels for (?) no charge, (?) 5 C/m^3,and (?) 10C/m^3

Figure 2 shows a cross section of the predicted semi hollow-cone spray structures taken through the centreline of the fuel injector at 1 ms aSOI. The results are showed only half of the spray because of the axial symmetry while predicted cross section of the spray through the centreline represents the most of liquid phase. The core spray penetration and angle at higher

gas pressure is significantly reduced as compared with that at low pressure due to the greater drag force.

The effect of electrostatic atomization is increased with increasing electric charge levels. The electric charge changes the surface tension at the leading edge of the spray thus promoting atomisation which in turn leads to the higher spray evaporation rate due to the increased fuel surface area. At the leading edge of the spray, where the fast moving droplets are entrained by the surrounding air around the outer edge of the spray cone. An increased number of smaller droplets are formed but then induced back into the spray cone.

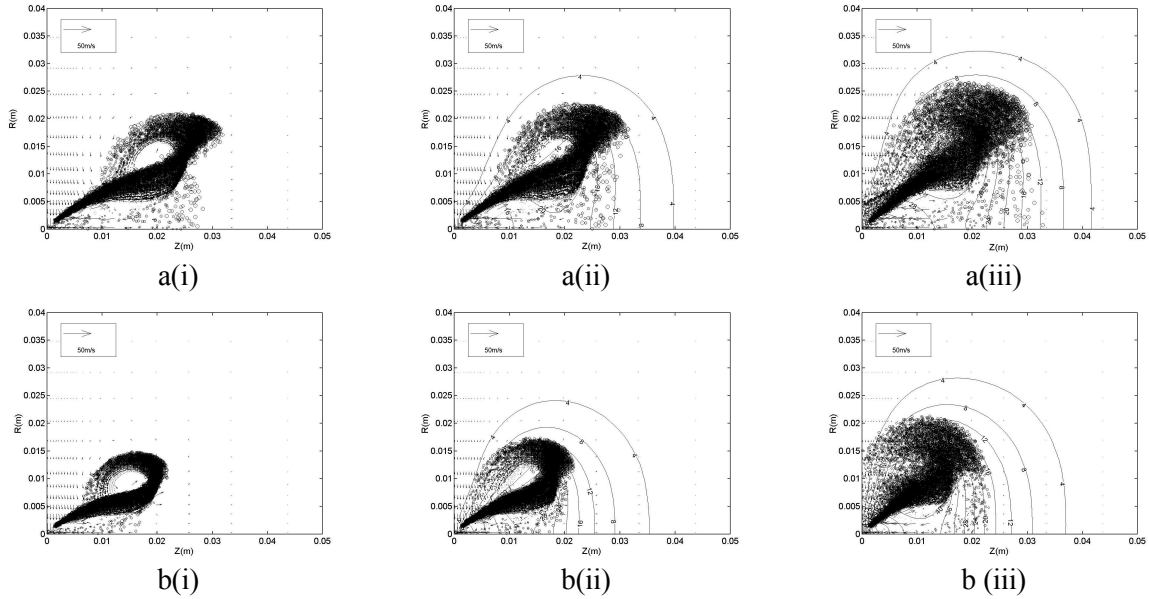

Fig. 2 Predicated semi hollow-cone spray structures with cross section through the centreline of the orifice showing break-up spray for (a) P_o = 1 bar, and (b) P_o = 6 bar with charge levels for (i) no charge, (ii) 5 C/m^3, and (iii) 10 C/m^3 at 1 ms aSOI

7. Conclusion

It is demonstrated that the use of electric charge may be used as a spray tuning tool in the high ambient pressures. The electric charge seems to increase the probability of droplets being re-entrained at the leading edge of the spray. As larger drops are produced by typical pressure-swirl atomizers [3] at higher ambient pressures, therefore, the use of electric charge may reduce the droplet size and maintain the desired spray structure at high gas pressures or with a late injection strategy. The optimal electric charge of 10 C/m^3 is recommended since it does not drive too much liquid onto the cylinder wall. With this electric charge level, the evaporation timescale can be as short as 3ms aSOI which is equivalent to an absolute time interval (i.e. time difference between the ignition time and start of injection timing) as that achieved when injecting late at an engine speed of 3000 rpm [3].

8. Appendix: Discrete single-component liquid droplet evaporation model

8.1. Momentum/position

Considering transient motion of a spherical particle with single liquid component within a much lower density ambient continuum, the drop has an electric charge, Q, and the electrical field, E_i. It is assumed that Basset force, gravity, and the force due to fluid pressure gradient are negligible, therefore, the motion of droplet through the surrounding is a function of the

Drag force and electrical body forces only. With this assumption the Lagrangian form of droplet momentum equation is expressed as:

$$\frac{dv_i}{dt} = \frac{u_i - v_i}{t_d} + \frac{QE_i}{m} \qquad : \qquad \frac{dx_i}{dt} = v_i \tag{12}$$

where u_i and v_i are the velocity of continuum and particle respectively, t_d is momentum time scale and is defined

$$t_d = \frac{r_d D^2}{18 m_G f_1} \tag{13}$$

where r_d and D and is density and diameter of droplet respectively, m_G is viscosity of the continuum and f_1 is empirical correction to Stroksian Drag for particle motion in the non-creeping flow regime [18]

$$f_1 = 1 + \frac{2}{3} Re_d^{2/3} \tag{14}$$

where $Re_d = r_G w D / \mu_G$ is Reynolds number where r_G is gas density.

8.2. Energy

Convective heat transfer is a major cause of energy transfer at liquid-gas interface. The evaporation mode is the M4 model from [19] which is one of a basic heat-mass transfer analogy model. It is derived from the equilibrium of vapor mass fraction boundary condition at the surface of the droplet with respect to time. The Lagrangian energy equation can be expressed as

$$\frac{dT_d}{dt} = \frac{T_G - T_d}{t_T} + \frac{L}{Cp_L m}\left(\frac{dm}{dt}\right) \tag{15}$$

where dm/dt is mass transfer rate and is negative for evaporation. T_d and T_G is bulk temperature of droplet and continuum respectively, L is the latent heat of evaporation and C_p is heat capacity of the liquid phase. t_T is temperature time scale and is defined as

$$t_T = \frac{1}{6} \frac{r_d}{l_G} \frac{D^2}{Nu} \frac{Cp_L}{f_1 f_2} \tag{16}$$

where l_G is gas thermal conductivity and $f_2 = (1+B_T)^{-1}$ is a correction to heat transfer due to evaporation. The heat transfer number B_T is defined as

$$B_T = \frac{C_{pV}}{L}\left(T_G - T_d\right) \tag{17}$$

where Cp_V is bulk heat capacity at vapor mixture. The Nusselt number, Nu, [20] can be given as

$$Nu = 2 + 0.552 Re_d^{1/2} Pr_G^{1/3} \tag{18}$$

where $Pr_G = m_G Cp_G / l_G$, is gas Prandtl number and Cp_G is heat capacity of gas phase.

8.3. Mass

The mass transfer rate can be defined with the mass time constant, t_m as

$$\dot{m} = \frac{dm}{dt} = -\frac{m}{t_m} B_M \tag{19}$$

The mass time constant is derived as

$$t_m = \frac{1}{6}\frac{r_d}{r_G}\frac{D^2}{G_G}\frac{1}{f_1 Sh} \tag{20}$$

where G_G is the binary diffusion coefficient. Sherwood number is analogous to Nusselt number given as

$$Sh = 2 + 0.552\, Re_d^{1/2}\, Sc_G^{1/3} \tag{21}$$

where $Sc = m_G r_G / G_G$ is Schmidt number. The Spalding transfer number or mass transfer number, B_M are defined as

$$B_M = \frac{Y_s - Y_G}{1 - Y_s} \tag{22}$$

where Y_s and Y_G are mass fraction of the vapor at the droplet surface and gas phase respectively. With the equilibrium assumption, Y_s can be obtained as

$$Y_s = \frac{c_s}{c_s + (1 - c_s)\frac{M_G}{M_V}} \tag{23}$$

where $c_s = P_{sat}/P_G$ is the surface equilibrium mole fraction of the vapor while P_{sat} is droplet saturation pressure and P_G is gas pressure. M_G/M_V is the ratio of molecular weight of gas phase over vapor phase. The droplet and continuum properties could be obtained elsewhere [21-24].

9. References

[1] Zhao F, Lai M C and Harrington D L 1999 *Prog. Engng. Combut*. **25** 437-562
[2] Lienemann H and Shrimpton J 2003 *Proc ICLASS* Sorrento Italy
[3] Kashdan J S, Arcoumanis C A and Shrimpton J S 2002 *Atom. Spray* **12**, 4, 539-557
[4] Leuteritz U, Velji A and Bach E 2000 *SAE paper* 2000-01-2041
[5] Lehr W and Hitler W 1993 *J. Electrostatics* **30,** 433-440
[6] Shrimpton J S "Pulsed Charge Sprays, Application to DISI Engines during Early Injection" accepted *Int. J. Num. Meth. Eng*.
[7] Lord Rayleigh 1882 *Philos Mag* **14** 184-186
[8] Adamczewski I 1969 *Ionization, Conductivity and Breakdown in Dielectric Liquids* (London: Taylor and Francis)
[9] Hinze J O 1955 *AIChE J* **1** 3 289-295
[10] Reitz R D and Diwakar R 1986 *SAE paper* 860469, 860598
[11] Pilch M and Esdman C 1987 *Int J Multi Flow* **13**, 6, 741-757
[12] Taylor G I 1964 Proc. Royal Soc. A. **280**, 383-397
[13] Cerkanowicz A E 1981 *Conference Record IEEE-IAS-Annual Meeting* Philadelphia PA
[14] Crowley J M 1986 *Fundamentals of Applied Electrostatics* (New York: Wiley)
[15] Nouri J and Whitelaw J H 2001 *Exp. Fluid.* **31**, 4, 377-383
[16] Reynolds W C 1976 *Ann. Rev. Fluid. Mech*. **8**, 183-208
[17] Melcher J R 1981 *Continuum Electromechanics* (Cambridge, Mass: MIT press)
[18] Putnam A 1961 *ARS J.* **31** 1467
[19] Miller R S, Harstad, K and Bellan J 1998 *Int. J. Multi. Flow* **24** 1025-1055
[20] Ranz W E and Marshall W R 1952 *Chem. Engng. Prog.* **48** 141-146
[21] Cengel Y A and Boles 1994 *Thermodynamics* (New York: MCGraw-Hill)
[22] Rohsenow W M, Hartneett, J P, and Cho Y I 1998 *Handbook of Heat Transfer* (New York: McGraw-Hill)
[23] Poling B E, Prausnitz J M and O'Connell J P 2001 *The Properties of Gases and Liquids* (New York: McGraw-Hill)
[24] Yaw C L, Yang H C, Hopper J R and Cawley W A 1991 *Hydroc. Proces.* **1**, 103